

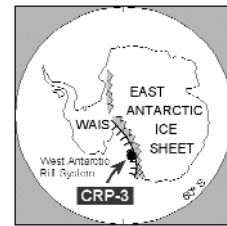
Petrophysics of Core Plugs from CRP-3 Drillhole, Victoria Land Basin, Antarctica

R.D. JARRARD

Dept. of Geology & Geophysics, 717 WBB, University of Utah, 135 S. 1460 East, Salt Lake City UT 84112-0111
(jarrard@mail.mines.utah.edu)

Received 28 October 2000; accepted in revised form 3 December 2001

Abstract - A suite of petrophysical properties - velocity, resistivity, bulk density, porosity, and matrix density - was measured on 88 core plugs from the CRP-3 drillhole. Core-plug bulk densities were used to recalibrate both whole-core and downhole bulk density logs. Core-plug measurements of matrix density permit conversion of the whole-core and downhole bulk density logs to porosity. Both velocity and formation factor (a normalized measure of resistivity) are strongly correlated with porosity. The velocity/porosity pattern is similar to that for the lower part of CRP-2A and is consistent with the empirical relationship for sandstones. Core-plug and whole-core measurements of P-wave velocity at atmospheric pressure exhibit excellent agreement. Measurements of velocity as a function of pressure indicate a significantly higher velocity sensitivity to pressure than has been observed at CRP-1 and CRP-2A; rebound or presence of microcracks at CRP-3 may be responsible. The percentage difference between velocities at *in situ* pressures and atmospheric pressures increases downhole from 0% at the seafloor to 9% at the bottom. This pattern can be used to correct whole-core velocity data, measured at atmospheric pressure, to *in situ* velocities for depth-to-time conversion and associated comparison to the seismic profile across the drillsite.



INTRODUCTION

The Cape Roberts Project (CRP) is an international drilling project whose aim is to reconstruct Neogene to Palaeogene palaeoclimate and the tectonic history of the Transantarctic Mountains and West Antarctic rift system, by obtaining continuous cores and well logs from a site near Cape Roberts, Antarctica. Offshore Cape Roberts, tilting and erosion of strata have brought Lower Miocene to Lower Oligocene sediments near the seafloor. The three CRP holes penetrate successively older portions of a 1600 m composite stratigraphic sequence. The third CRP drillhole, CRP-3, cored 821 m of Lower Oligocene and possibly Upper Eocene sedimentary rocks and 116 m of underlying Devonian sandstone (Cape Roberts Science Team, 2000). Average core recovery was 97%. The mid-Tertiary section consists primarily of sandstones and muddy sandstones; other lithologies include common thin conglomerate beds and less common sandy mudstones and diamictites (Cape Roberts Science Team, 2000).

Seismic velocity, density, and porosity of sediments drilled by the CRP can be determined in three ways: by whole-core measurements, by downhole logging, or by lab measurements on core plugs. Continuous whole-core measurements of bulk

density, compressional wave velocity (V_p), and magnetic susceptibility, as well as downhole measurements of density, neutron porosity, resistivity, V_p , magnetic susceptibility, and natural gamma radiation, were obtained at the rig site (Cape Roberts Science Team, 2000).

This study provides the third, complementary, data set: laboratory measurements of velocity versus pressure and of bulk density, porosity, matrix (or grain) density, and formation factor for 88 core plugs. Plug sampling, averaging 1 sample per 10 m, was intended to be representative of major lithologies, except that conglomerates were not sampled. Although core-plug measurements are made on smaller samples with different methods from whole-core and well-logging data, they can address issues critical to the analysis and interpretation of the well-log and whole-core measurements. These issues are:

- (1) Core-plug measurements can be used to calibrate well logs and to confirm the calibration of whole-core measurements.
- (2) What is the matrix density of the CRP-3 sediments? Matrix density is needed for conversion of well-log and whole-core densities to porosities.
- (3) Measurements of velocity versus pressure provide a bridge between *in situ* seismic velocities and laboratory-pressure whole-core measurements.

- (4) The velocity/porosity relationship can indicate petrophysical signatures of diagenesis and exhumation.

METHODS

In McMurdo Station, Antarctica, 97 cylindrical samples were drilled from the working halves of the CRP-3 cores; the circulating fluid used to remove cuttings was water. Sample diameters were 2.5 cm. Volumes of most samples were 6-13 cm³. Samples were sealed while saturated, to prevent drying and permit subsequent petrophysical measurements to be undertaken on water-saturated specimens. This sample handling contrasts with the CRP-1 and CRP-2A procedure of allowing samples to dry during palaeomagnetic measurements prior to petrophysical analyses, and later saturating samples with kerosene to avoid clay swelling (Brink & Jarrard, 1998, 2000). By keeping the samples water-saturated, we avoided ambiguities encountered by Brink & Jarrard (1998, 2000) concerning use of the Gassmann (1951) equation for converting kerosene-saturated velocities to those of seawater-saturated samples.

POROSITY AND DENSITY MEASUREMENTS

Porosity, bulk density, and matrix density of the core plugs (Tab. 1) were determined using a simple weight-and-volume technique, as described by Brink & Jarrard (1998) and Brink (1999), with salt correction (Hamilton, 1971a). Resistivity (Tab. 1) was measured with a two-electrode technique and 1-kHz, 50-mV alternating current, as described by Jarrard & Schaar (1991). Several samples were unsuitable for some types of measurement, due to inadequate consolidation, cracks, or non-cylindrical shape.

VELOCITY MEASUREMENTS

Velocities of water-saturated samples (Tab. 2) were measured in a New England Research velocimeter, as described by Brink & Jarrard (1998) and Brink (1999). Pore pressures were kept atmospheric, so confining pressure was equal to differential pressure. Measurements of velocity at atmospheric pressure are usually not representative of *in situ* velocities for two reasons: reduced interparticle coupling and microcrack opening. These effects can be reversed by measuring the samples at *in situ* pressures. Modern *in situ* lithostatic pressures for these CRP-3 sediments range between 0.6 and 9.5 MPa.

Because poorly lithified sediments may deform viscoelastically or lose rigidity at fairly modest pressures, Brink & Jarrard (1998) measured velocities of CRP-1 samples on both upgoing and downgoing pressure cycles. CRP-2A and CRP-3 sedimentary rocks are more lithified than those from CRP-1. Brink

Tab. 1 - Petrophysical measurements.

Depth (mbsf)	Bulk density (kg/m ³)	Porosity (%)	Matrix density (kg/m ³)	Resistivity (ohm*m)	Formation factor
49.56	1959	41.5	2622	1.2	6.4
60.91	1981	41.2	2653	1.3	7.1
69.58	1990	41.3	2671	1.3	7.1
81.12	2122	35.1	2718	1.5	7.8
90.54	2221	28.3	2692	2.2	11.3
119.53	2245	26.2	2677	3.1	16.4
129.72	2153	28.4	2600	3.0	15.9
134.06	2205	28.3	2672	3.6	19.0
141.79	2222	26.2	2646	3.8	20.0
151.22	2425	16.3	2698		
155.03				2.0	10.3
165.74	2263	24.0	2654	4.6	24.4
169.83	2404	16.0	2667	9.5	50.0
177.82	2291	21.6	2640	5.7	29.9
185.07	2350	19.0	2661	6.5	34.4
194.82	2240	25.1	2647	7.1	37.2
207.52	2251	23.5	2628	7.3	38.5
213.10	2366	15.0	2603	11.4	60.0
223.15	2462	11.7	2653	12.9	68.0
234.43	2201	27.2	2640	3.7	19.6
243.02	2224	24.5	2614	4.0	21.0
250.67	2296	22.5	2664	5.2	27.6
269.64	2274	24.4	2678	2.8	15.0
278.63	2276	22.2	2634	3.9	20.4
286.24	2128	29.7	2594	2.6	13.7
295.85	2491	11.9	2689	12.8	67.1
311.95	2269	23.6	2655	5.4	28.3
316.97	2372	16.0	2629	11.2	59.0
323.62	2341	19.0	2649	6.7	35.3
332.63	2136	30.0	2613	2.4	12.5
337.92	2414	13.2	2625	8.8	46.2
344.04				3.1	16.1
354.88	2167	28.3	2617	2.5	13.0
361.37	2291	21.7	2642	4.6	24.4
369.57	2496	9.1	2642	10.3	54.4
374.19	2245	26.8	2693		
399.65				3.5	18.6
409.87	2356	19.4	2675	6.1	31.9
427.59				2.1	10.9
437.61	2198	26.4	2618	3.9	20.7
457.78	2228	27.4	2682	3.4	17.7
463.85	2171	23.9	2531	3.7	19.4
470.86	2193	26.5	2614	2.5	13.0
476.71	2175	29.5	2655	2.3	12.3
489.24	2195	25.9	2603		
491.88	2207	29.6	2703	2.4	12.9
513.53	2261	23.5	2640		
520.36	2182	27.5	2620	3.4	17.8
533.88	2544	8.6	2687	13.4	70.3
541.79	2292	21.6	2641	5.5	28.9
545.81	2290	23.6	2681	4.1	21.4
557.52	2256	23.1	2627	4.4	23.0
573.94				3.8	20.1
581.59	2301	20.1	2622	4.3	22.8
593.38	2222	25.4	2631	3.4	17.8
603.38	2248	24.8	2653	3.2	16.9
615.87	2120	29.6		3.9	20.3
627.77	2407	17.1	2693	11.0	58.1
636.06	2202	26.9	2635	3.3	17.1
645.40	2309	21.7	2664	4.6	24.4
649.51	2249	26.1	2682	3.8	19.9
665.16	2253	23.5	2631	4.8	25.1
676.14	2304	22.3	2670	5.3	27.7
682.67	2236	27.4	2693	3.3	17.2
685.82	2207	24.9	2599	3.4	18.1
692.32	2216	26.1	2638	3.2	16.8
700.38	2253	24.5	2652	3.6	19.1
710.50	2429	15.8	2694	7.9	41.7
714.83	2323	17.9	2606	5.8	30.3
721.29	2274	25.4	2701	4.1	21.4
728.36	2370	17.0	2645	8.3	43.5
734.82	2364	18.4	2667	6.6	34.5
740.94	2296	23.9	2696	4.2	22.2
744.54	2194	26.4	2614	3.7	19.7
750.25	2277	27.5	2752	3.3	17.4
758.55	2314	19.9	2635	5.6	29.7
763.23	2296	19.9	2612	5.1	26.9
766.25	2303	20.4	2630	5.6	29.6
778.52	2284	20.4	2607	4.6	24.2
786.41	2374	17.7	2665	6.8	35.9
828.22	2280	24.8	2695	4.6	24.4
844.95	2351	15.5	2594	5.7	30.0
864.84	2348	15.8	2596	5.4	28.4
881.00	2418	12.8	2622	7.4	38.7
894.65	2264	21.6	2605	3.2	16.7
910.17	1990	45.0	2780	1.4	7.5
925.08	2285	19.5	2591	3.7	19.2
939.02				3.3	17.4

Tab. 2 - CRP-3 velocity measurements.

Depth (mbsf)	V _{atm} (m/s)	V _{in situ} (m/s)	Original (m/s)	Patm (MPa)	P _{in situ} (MPa)	Original (MPa)	V _p /V _s in situ	V _{in situ} /V _{atm} %	Original/V atm %
60.91	1998	1998	2227	0.69	0.69	8.3			111.5
69.58	2024	2024	2197	0.69	0.69	8.3			108.5
81.12	2165	2165	2445	0.86	0.86	8.4	1.73		112.9
90.54	2470	2490	2713	0.69	0.86	8.4		100.8	109.8
119.53	2822	2842	2937	0.69	1.2	8.8		100.7	104.0
129.72	2685	2709	2811	0.69	1.4	8.9		100.9	104.7
134.06*	2916	2820	2954	0	1.7	10.3	1.76	96.7	101.3
141.79	3080	3086	3110	0.69	1.4	8.9		100.2	101.0
155.03			2793			9.1			
165.74	3266	3263	3256	0	1.7	9.3		99.9	99.7
169.83*	3944	3962	3928	0	1.7	10.3	2.11	100.4	99.6
177.82	3396	3447	3495	0	1.9	9.5		101.5	102.9
185.07	3461	3562	3569	0	1.9	9.5	1.97	102.9	103.1
194.82	3089	3159	3319	0	2.1	9.6	1.87	102.2	107.4
207.52	3277	3343	3422	0	2.1	9.6		102.0	104.4
213.10	3900	4065	4094	0	2.2	9.8		104.2	105.0
223.15	4412	4431	4595	0.69	2.2	9.8		100.4	104.1
234.43	2761	2968	3039	0	2.4	10.0		107.5	110.1
243.02	3069	3075	3155	0	2.4	10.0		100.2	102.8
250.67	3290	3356	3457	0.69	2.6	10.1		102.0	105.1
269.64	2743	2980	2971	0	2.8	10.3		108.6	108.3
286.24	2910	2916	2982	0.69	2.9	10.5		100.2	102.5
295.85	4249	4372	4383	0	3.1	10.7		102.9	103.2
311.95	3277	3287	3307	0.69	3.3	10.8	1.91	100.3	100.9
316.97	3720	3871	3891	0	3.3	10.8		104.1	104.6
323.62	3439	3558	3602	0	3.4	11.0	1.98	103.5	104.7
332.63			2837			3.4			
337.92	3685	3750	3798	0	3.4	11.0		101.8	103.1
344.04	2694	2738	2813	0.69	3.4	11.0		101.6	104.4
354.88	3011	3066	3194	0	3.6	11.2		101.8	106.1
361.37	3116	3387	3479	0	3.8	11.4		108.7	111.6
369.57	3834	4237	4388	0	3.8	11.4		110.5	114.4
409.87	3429	3494	3518	0.69	4.1	11.7	2.17	101.9	102.6
437.61	3100	3296	3349	0	4.5	12.0		106.3	108.0
463.85	3068	3196	3312	0.69	4.8	12.4	2.01	104.2	108.0
470.86	2535	2583	2633	0	4.8	12.4		101.9	103.9
476.71	2863	2991	3134	0.69	4.8	12.4		104.4	109.5
491.88		2836	2920			5.2			
520.36	2732	2933	3041	0.69	5.3	12.9		107.4	111.3
533.88	4558	4795	4790	0.69	5.5	13.1		105.2	105.1
541.79	3527	3631	3686	0.69	5.5	13.1		102.9	104.5
545.81	3589	3786	3919	0.69	5.7	13.2		105.5	109.2
557.52	2713	2865	2899	0.69	5.7	13.2		105.6	106.8
593.38*	2155	2281	2285	0.69	6.9	13.8		105.9	106.0
603.38	2793	3053	3182	0.69	6.2	13.8		109.3	113.9
615.87		2896	2943			6.4			
627.77*	4000	4215	4259	0	6.9	13.8		105.4	106.5
636.06	2939	3054	3101	0.69	6.5	14.1	2.02	103.9	105.5
645.40	3558	3742	3803	0.69	6.5	14.1		105.2	106.9
649.51	2987	3368	3395	0	6.5	14.1		112.8	113.7
665.16	3312	3460	3502	0.69	6.9	14.4		104.5	105.7
685.82	3018	3218	3274	0.69	7.1	14.6	2.02	106.6	108.5
692.32	2691	2900	2992	0.69	7.1	14.6		107.8	111.2
710.50	3843	4254	4345	0.69	7.2	14.8		110.7	113.1
714.83	3549	3825	3853	0.69	7.4	15.0		107.8	108.6
721.29	2953	3225	3262	0	7.4	15.0		109.2	110.4
728.36	3884	4096	4124	0.69	7.4	15.0		105.5	106.2
734.82	3749	3847	3877	0.69	7.6	15.1	2.03	102.6	103.4
740.94	3283	3541	3597	0.69	7.6	15.1		107.8	109.5
744.54	2840	3072	3128	0.69	7.6	15.1		108.1	110.1
750.25	2871	3177	3243	0.69	7.7	15.3		110.6	112.9
758.55	3318	3583	3635	0.69	7.7	15.3		108.0	109.6
763.23	3184	3425	3544	0.69	7.7	15.3		107.6	111.3
766.25	3456	3712	3747	0.69	7.9	15.5		107.4	108.4
786.41	3828	3996	3917	0.69	8.1	15.7		104.4	102.3
828.22	3304	3408	3402	0.69	8.4	16.0		103.1	103.0
844.95	3752	3788	3849	0.69	8.6	16.2	2.33	100.9	102.6
864.84*	3715	4108	4182	0	6.9	17.2	1.87	110.6	112.6
881.00	4177	4441	4450	0.69	9.1	16.7	1.92	106.3	106.5
894.65	3275	3526	3756	0.69	9.2	16.7	1.81	107.7	114.7
925.08*	3581	3849	3932	0.69	9.5	17.1	1.95	107.5	109.8

*complete measurement series

& Jarrard (2000) used a similar approach for four representative samples from CRP-2A. For six samples from CRP-3, we used the following pressure steps: 0, 0.69, 1.7, 3.4, 5.2, 6.9, 10.3, 13.8, and 17.2 MPa. To determine the pressure dependence of any rigidity loss, we alternated each increased-pressure increment with a return to low pressure (0.69 MPa) for remeasurement. Whereas most CRP-1 samples had exhibited substantial rigidity loss and associated 5-14% velocity reduction at pressures of 10.3-17.2 MPa (Brink & Jarrard, 1998), only the shallowest of the four CRP-2A samples (from 115 mbsf, within the CRP-1 depth range) exhibited this pattern (Brink & Jarrard, 2000). None of the CRP-3 samples exhibits evidence of either rigidity loss or velocity increase (< 2% velocity change), even after exposure to high

pressure (17.2 MPa). We conclude that most CRP-2A samples and all CRP-3 samples are sufficiently consolidated to be free of rigidity loss.

For these pilot CRP-3 samples, we found that 10 minutes was enough time to allow the pressure within the samples to equilibrate: little or no velocity change was observed after allowing times from 20 minutes to 24 hours to elapse between several of the consecutive measurements. Consequently, we waited a minimum of 10 minutes between velocity measurements at different pressures for all subsequent CRP-3 measurements.

Based on these results, routine velocity measurements were made in 3-4 steps. Velocity was first measured at a differential pressure 7.6 MPa higher than present *in situ* differential pressure, then at *in situ* differential pressure (based on 10 MPa/km). The final pressure step was 0 MPa or – if transducer coupling was inadequate at this pressure – at 0.69 MPa. Occasionally, slightly higher pressures were needed to obtain sufficient transducer coupling for accurate velocity measurement. Table 2 lists V_p results of all samples that exhibited adequate coupling for useful measurements. Shear-wave measurements were also made at each V_p step, but only a few of these waveforms have been analyzed and presented in table 2. Because the bottom half of the hole was cored with smaller-diameter drill rod than the top half, core plugs were correspondingly shorter: generally 16-20 mm for the deeper cores vs. 25-28 mm for the shallow cores. We found that it was usually difficult to distinguish converted P-waves from S-waves in the shortest samples, and we suspect that a similar problem was present but not recognized in some of the CRP-2A V_s results of Brink & Jarrard (2000).

POROSITY INFLUENCE ON PETROPHYSICAL PROPERTIES

DENSITY

Continuous CRP-3 logs of bulk density as a function of depth are available from both whole-core measurements (Cape Roberts Science Team, 2000) and well logging (Cape Roberts Science Team, 2000; Bückler et al., this volume). These density logs can be converted to porosity by assuming a constant matrix density and applying the relationship $\rho_b = \phi\rho_f + (1-\phi)\rho_{ma}$, where ρ_b is bulk density, ϕ is fractional porosity, ρ_f is fluid density (1024 kg/m³), and ρ_{ma} is matrix density. The 2648 kg/m³ mean matrix density for CRP-3 (Tab. 1) is nearly identical to the expected value of 2650 for pure quartz, but significantly less than the means of 2720 kg/m³ for CRP-2A (Brink & Jarrard, 2000) and 2700 kg/m³ for CRP-1 (Brink & Jarrard, 1998). Beacon sandstones, which contain a significant fraction of lower matrix-density feldspar,

appear to have a slightly lower average matrix density of 2640 kg/m^3 . The low standard deviation of measured matrix densities (40 kg/m^3) indicates that the assumption of uniform matrix density introduces negligible errors into the conversion from density to porosity.

RESISTIVITY AND FORMATION FACTOR

The CRP-3 shallow-resistivity log contains the most detailed character of the three resistivity curves and demonstrates negligible influence from conductive borehole fluids. Shallow resistivity was converted to formation factor to eliminate the effect of pore water conductivity: $FF = R_o / R_w$, where FF is formation factor, R_o is formation resistivity, and R_w is resistivity of the pore fluid (100% water). Changes in pore-fluid resistivity versus depth were determined by calculating R_w from a temperature log and seawater salinity. Similarly, core-plug resistivities were converted to formation factors, using lab measurements of R_w (Tab. 1). A crossplot of porosity versus natural logarithm of formation factor for core-plug data (Fig. 1A) shows that formation factor is strongly dependent on porosity ($R = -0.87$), as expected for sandstones (Archie, 1942). For clean sandstones, the modified Archie equation is $FF = a/\phi^m$, where a and m are empirically determined local constants. Linear regression (excluding the two lowest-porosity points) provides estimates of $a=1.8$ and $m=1.7$ which can be used to convert the formation-factor log to a porosity log. Our estimated value of a is significantly higher than most results for sandstones (*e.g.*, Keller, 1989) but similar to that obtained for Miocene sands by Porter & Corothers (1971).

Devonian Beacon sandstones appear to have significantly lower formation factors, for a given porosity, than the Tertiary sandstones (Fig. 1A), but too few Beacon points are available for determination of separate Beacon and Tertiary trends. This difference in formation factors is also evident in a crossplot of formation factor vs. P-wave velocity (Fig. 1B), where atmospheric-pressure velocities are used since formation factors are measured at atmospheric pressure. In contrast, comparison of Beacon and Tertiary responses on a velocity/porosity crossplot (not shown) detects no differences. The distinction between Beacon and Tertiary responses is not simply a depth-varying effect, as the deepest and shallowest Tertiary samples exhibit similar petrophysical behavior (except for gradual pressure-dependent effects discussed in a later section). Both velocity and formation factor respond to porosity and cementation. However, formation factor is more sensitive to pore geometry than is velocity. Apparently, pore geometry is more open and continuous in the Beacon sandstones than in the Tertiary sediments. Either pore-lining authigenic clays in the Tertiary sandstones (Wise et al., this volume) or secondary porosity in the Beacon may be responsible for this difference.

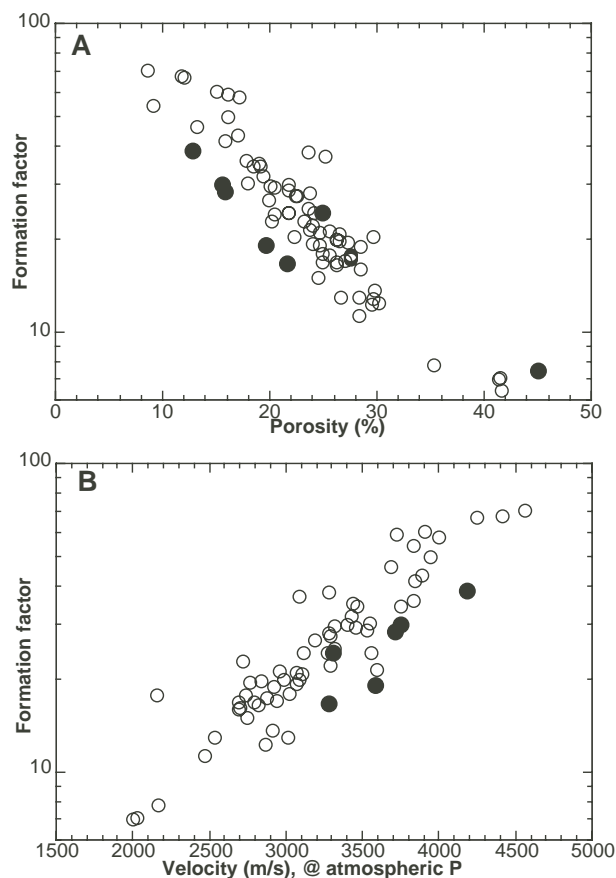


Fig. 1 - A: Relationship between formation factor and porosity. B: Relationship between formation factor and velocity. Open circles: Tertiary shelf samples; solid dots: Devonian Beacon samples.

VELOCITY

Velocity is strongly correlated with porosity for the CRP-3 sediments (Fig. 2). Such a relationship is expected from Gassmann's (1951) theoretical model for the controls on velocity in porous rocks: porosity is explicitly included in this model, but it implicitly affects velocity also through its influence on frame bulk modulus (Hamilton, 1971b), shear modulus (Stoll, 1989), and bulk density. Consequently, siliciclastic rocks and sediments from all parts of the world exhibit a strong dependence of V_p on porosity (*e.g.*, Wyllie et al., 1958; Erickson & Jarrard, 1998).

The second-order control on velocity is shale percentage for siliciclastic sedimentary rocks with porosities of less than $\sim 30\%$, whereas consolidation state is more important in higher-porosity sediments (Erickson & Jarrard, 1998). Because CRP-3 porosities bracket the porosity range at which a transition of second-order controls is expected, both shale percentage and consolidation state may affect CRP-3 velocities. CRP-2A data demonstrate the influence of consolidation state on the velocity/porosity pattern: plug results from the more cemented bottom half of the hole define a higher velocity/porosity trend than those from the top half, and local departures from the average velocity/porosity relationship are well correlated with cementation (Jarrard et al., 2000).

Figure 2 compares the velocity/porosity pattern for CRP-3 samples to the deeper CRP-2A results (Brink & Jarrard, 2000) and predicted empirical trends (Erickson & Jarrard, 1998). The CRP-2A measurements shown are at *in situ* pressures, and the CRP-3 data are at original, pre-exhumation pressures. CRP-3 velocities exhibit a velocity/porosity pattern consistent with that for deep CRP-2A samples. The CRP-3 samples are nearly all sandstones or muddy sandstones, so we compare them to the sandstone and muddy sandstone (20% shale, 80% sandstone) empirical trends. Below a critical porosity (Nur et al., 1991) of about 31%, both CRP datasets are compatible with the expected empirical trend. Above 31% porosity, deep CRP-2A results are systematically higher than predicted for the normal-consolidation model (Fig. 2), because this interval is more cemented than is typical for such high-porosity sediments (Jarrard et al., 2000).

PRESSURE INFLUENCE ON PETROPHYSICAL PROPERTIES

REBOUND, MICROCRACKS, AND EXHUMATION

Velocity at atmospheric pressure is usually lower than *in situ* velocity for three reasons: reduced interparticle coupling, rebound, and microcrack opening. Overburden pressure increases the number and area of interparticle contacts, thereby increasing shear modulus and frame bulk modulus; this increased framework stiffness increases velocity (Stoll, 1989). Rebound is the expansion that unconsolidated sediments undergo when removed from *in situ* pressures (Hamilton, 1976). For uncemented terrigenous sediments, porosity rebound commonly increases from near-zero for sea-floor sediments to ~4-6% at 500-600 mbsf (Hamilton, 1976). Below this depth, rebound often decreases because of incipient cementation. Velocity rebound is larger than porosity rebound, because of reduced sediment strength, so rebound lowers the entire pattern of velocity dependence on porosity (Jarrard et al., 1989; Erickson & Jarrard, 1998).

Brink & Jarrard (2000) concluded that CRP-2A petrophysical responses indicate much less rebound than is typical of normally compacted, unconsolidated sediments. Porosity rebound at CRP-2A is negligible, based on agreement of both core-plug and whole-core densities with *in situ* densities (Brink & Jarrard, 2000; Bucker et al., 2000). Their measurements of velocity vs. pressure demonstrate that velocity rebound is surprisingly low, averaging only 1-2%. They suggested that rebound is suppressed by the extensive cementation at CRP-2A.

Another factor that can affect petrophysical responses is the opening of microcracks by exhumation, the removal of overburden. Most rocks exhibit patterns of increasing V_p with increasing pressure, attributable to closing of microcracks (*e.g.*,

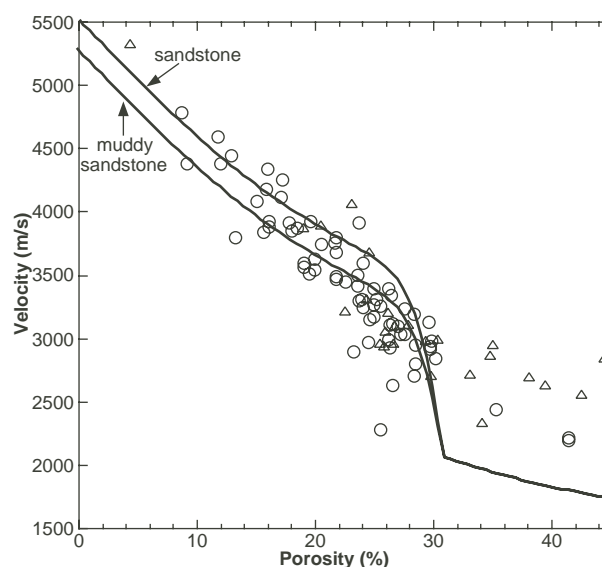


Fig. 2 - CRP velocity-porosity relationship based on core plugs. Open circles: CRP-3 data of Tables 1 & 2, at original (pre-exhumation) pressures; open triangles: CRP-2A data from deeper than 325 mbsf, at *in situ* pressures. Also shown (solid lines) are empirical relationships (Erickson & Jarrard, 1998) for normally compacted sandstone and muddy sandstone.

Nur, 1971; Bourbié et al., 1987). Initial microcrack porosities of <0.5% are sufficient to cause pressure-dependent velocity variations of 5-50%, indicating that the primary effect of pressure on velocity is through its impact on frame bulk modulus, not on porosity or density (Walsh, 1965; Nur & Murphy, 1981; Bourbié et al., 1987). CRP-3 velocities increase with increasing pressure (Fig. 3A) in a manner typical of microcracked rocks (*e.g.*, Bourbié et al., 1987). This pattern contrasts with the nearly flat velocity/pressure behavior, inconsistent with microcracking, observed for samples from CRP-1 and CRP-2A (Brink & Jarrard, 1998, 2000).

Compaction patterns at CRP-2A indicate only about 250 m of exhumation (Brink & Jarrard, 2000), and stratigraphic correlation between CRP-2A and CRP-1 indicates even less exhumation at CRP-1. In contrast, stratigraphic correlation between CRP-2A and CRP-3 (Cape Roberts Science Team, 2000), adjusted for lateral thinning of sequences, indicates *ca.* 750 m of exhumation at CRP-3. Consequently, the pressure responses for CRP-3 may contrast with those for CRP-2A.

Exhumation-induced microcracking may account for the much greater velocity response at CRP-3 than at CRP-2A. Stress relief at CRP-3 may also account for differences in modern stress magnitudes at the two sites (Jarrard et al., this volume). Within CRP-3, the sensitivity of velocity to pressure increases downcore (Fig. 3A). Figure 3B plots the percentage difference between *in situ* measurements and atmospheric-pressure measurements versus depth. *In situ* velocities are systematically higher than those measured at atmospheric pressure, with a difference that rises from 0% at 0 mbsf to 9% at the bottom of

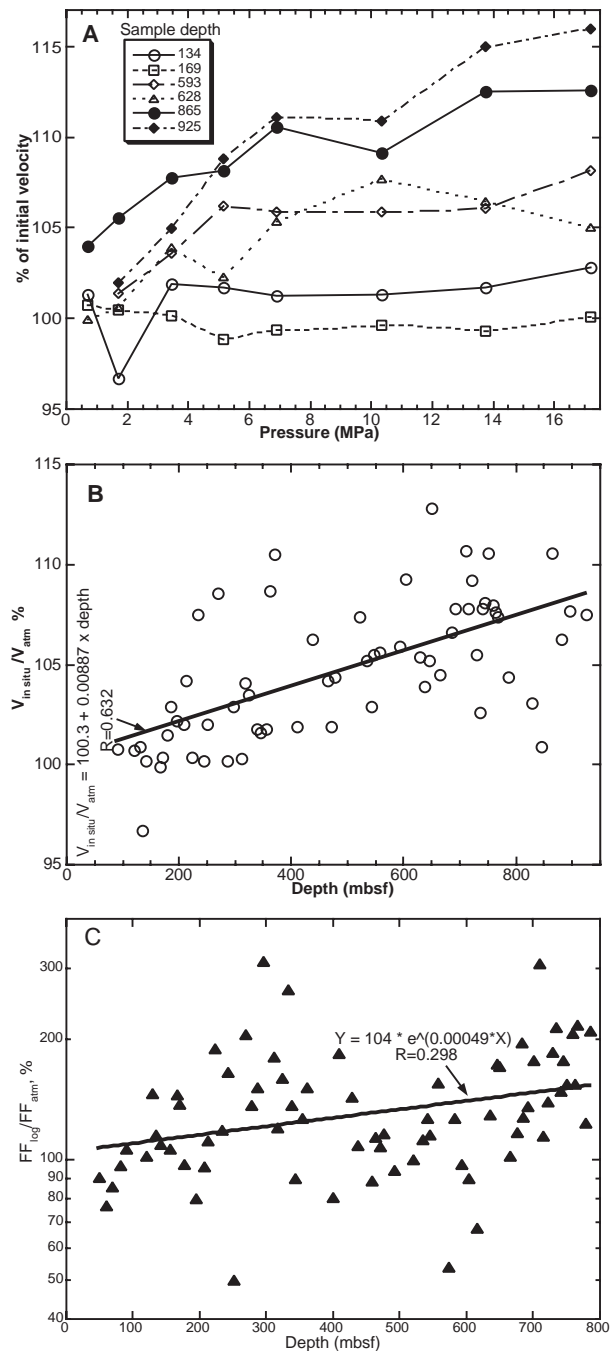


Fig.3 - Effects of burial pressure on CRP-3 petrophysical responses. A: measurements of velocity as a function of pressure, for 6 pilot samples. Note the increased sensitivity of velocity to pressure for samples from greater depth. B: percentage difference between velocities measured at atmospheric and *in situ* pressures, as a function of depth. The discrepancy increases with depth as shown by the linear fit. C: percentage difference between atmospheric-pressure core-plug measurements and *in situ* well-log measurements of formation factor.

the hole. This pattern is compatible with either rebound or a depth-dependent increase in microcracking.

If the downhole increase of pressure-dependent velocity behavior is caused by rebound, then porosity rebound should also be present. Porosity rebound is potentially detectable by comparing atmospheric-pressure measurements of either density or formation

factor to *in situ* measurements. Unfortunately, one cannot test for rebound by comparing the density well log to the whole-core density log, because the former is calibrated to the latter (Bücker et al., this volume). It is possible, however, to test for rebound by comparing core-plug measurements of formation factor to the formation-factor well log (Fig. 3C). Variance is high, due to stratigraphic heterogeneity and the difference in sampling volumes, but a weak dependence of formation-factor rebound on depth is apparently detectable. At 800 mbsf, *in situ* formation factors are ~50% higher than those at laboratory pressure, a difference that implies ~4 porosity units of rebound, based on the relationship between formation factor and porosity in figure 1. The relationship between velocity and porosity (Fig. 2) suggests that a 4 porosity-unit increase implies ~7-8% velocity decrease, similar to that observed at 800 mbsf (Fig. 3B). Thus it appears that rebound is generally compatible with all of the pressure-dependent petrophysical responses of figure 3.

IMPLICATIONS FOR IN SITU VELOCITIES

Core-plug velocities measured at atmospheric pressure can provide an independent confirmation of the reliability of whole-core measurements. It does not follow, however, that whole-core measurements can be used directly for linking CRP-3 depths to seismic time. Our measurements of velocity versus pressure provide an indication of the likely differences between *in situ* velocities and those measured on continuous cores at laboratory pressure. For estimation of seismic reflector depths based on whole-core velocities (Cape Roberts Science Team, 2000; Henrys et al., this volume), these velocities should be increased by the depth-dependent function shown in figure 3B. Henrys et al. (this volume) find that variations in uncorrected CRP-3 whole-core velocities are similar in character to those of interval velocities from a vertical seismic profile, but the latter are subtly faster in the bottom half of the hole.

CORE-PLUG CALIBRATION OF WHOLE-CORE AND WELL-LOG DATA

COMPARISON TO WHOLE-CORE DATA

Figure 4 compares core-plug measurements of velocity and density to the whole-core results of Cape Roberts Science Team (2000). Most of the whole-core spikes to high velocity and density are conglomerates, not sampled for core-plug measurements because heterogeneity is too high for plugs to be representative. Because whole-core measurements were made at atmospheric pressure, atmospheric-pressure core-plug velocities are displayed.

Agreement between whole-core and plug velocities is generally excellent; this agreement is more obvious

on plots of short depth intervals than on the composite plot of figure 4. The only exception to this generalization is that the five Beacon plug results (deepest points on figure 4) may be systematically slightly faster than whole-core velocities, but too few points are available to be certain.

Whole-core and plug densities, in contrast, do not agree. Whole-core densities are systematically higher, by 2-8%, than plug densities (Fig. 4A). We cannot account for this small but significant discrepancy. Both measurement techniques used standards as a confirmation of reliability. A further confirmation of the plug densities is the very tight clustering of plug matrix densities at a value appropriate to quartz. Porosity/velocity patterns can be used to demonstrate that the discrepancy results from depth-dependent biases within the whole-core dataset. As previously discussed, core-plug data from all depths define a single porosity/velocity trend that is consistent with empirical relationships (Fig. 2). In contrast, when whole-core densities are converted to porosities and plotted *vs.* velocity, sudden offsets of the entire porosity/velocity trend are evident at 120, 345, 503, and 833 mbsf, and all five porosity/velocity trends are inconsistent with empirical relationships. By comparing each of these trends to the core-plug

relationship, the whole-core density biases can be estimated: 120 kg/m³ for <120 mbsf, 60 kg/m³ for 120-345 mbsf, 220 kg/m³ for 345-503 mbsf, 110 kg/m³ for 503-833 mbsf, and 170 kg/m³ for >833 mbsf. We recalibrated the whole-core density record by removing these biases (Fig. 5B).

CORE-PLUG RECALIBRATION OF THE DENSITY WELL LOG

The density well-logging tool, which determines bulk density by measuring gamma-ray attenuation, was calibrated initially by comparison to whole-core densities (Cape Roberts Science Team, 2000; Bucker et al., this volume). Because plug densities indicate bias in the original whole-core densities, a recalibration of the density log is warranted. This recalibration does not affect the multivariate statistical analyses of Bucker et al. (this volume), because those analyses use standardized logs.

Figure 5 illustrates the effects of recalibrating the whole-core and downhole density logs, concentrating on a relatively short 200 m interval to permit a more detailed comparison than is possible from simultaneous examination of the entire record (*e.g.*, Fig. 4). Before recalibration, the whole-core and well-

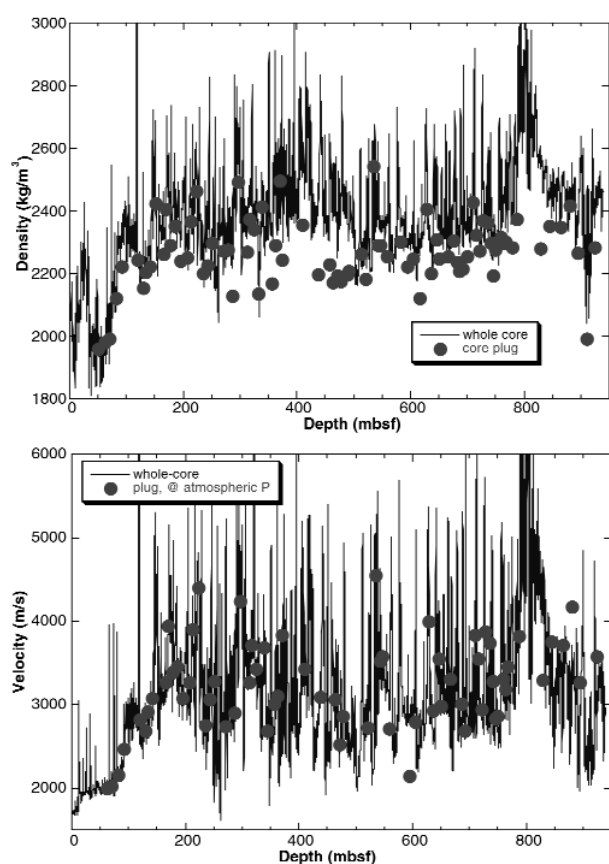


Fig. 4 - Density and velocity records obtained by whole-core measurements (Cape Roberts Science Team, 2000), compared to core-plug data (solid dots) of this study. Both plug and whole-core velocities are measured at atmospheric pressure. Note the systematic discrepancies for density, in contrast to good agreement for velocity.

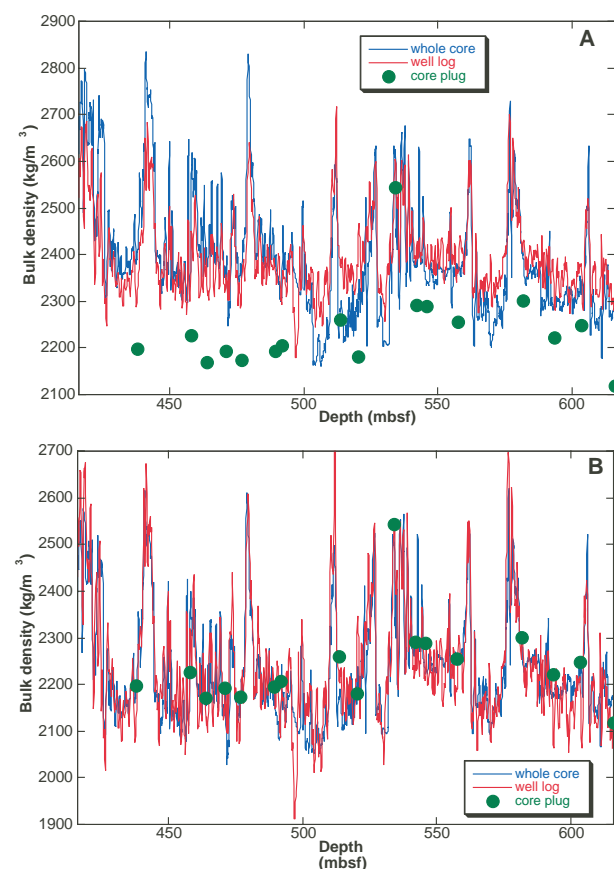


Fig. 5 - Comparison of three suites of bulk density measurements: whole-core (Cape Roberts Science Team, 2000), well logs calibrated to whole-core data (Bucker et al., this volume), and core plugs of this study. Top: before recalibration to core plugs; bottom: after recalibration. For clarity, only a 200-m interval of the 939-m CRP-3 drillhole is shown.

log densities generally agree, as expected because the latter was calibrated with the former. However, well-log data are systematically higher than whole-core data below ~500 mbsf, and this pattern is reversed above ~500 mbsf. In addition, well-log peak-to-trough amplitudes are smaller than those for whole core. Recalibration to core-plug data not only gives an excellent match of both well-log and whole-core data to the plug results, but also significantly improves the match between well-log and whole-core data.

ACKNOWLEDGEMENTS - I sincerely thank Gary Wilson, Fabio Florindo, Leonardo Sagnotti, and Adam Harris for taking the samples analyzed here. This research was supported by the National Science Foundation (OPP-9418429).

REFERENCES

- Archie G.E., 1942. The electrical resistivity log as an aid in determining some reservoir characteristics. *Trans. Amer. Inst. Mineral Met.*, **146**, 54-62.
- Bourbié T., Coussy O. & Zinszner B., 1987. *Acoustics of Porous Media*. Ed. Tech., Paris, 334 p.
- Brink J.D., 1999. *Petrophysics and Log-based Sedimentology of the Cape Roberts Project, Antarctica*. Univ. of Utah, unpubl. M.S. thesis, 183 p.
- Brink J.D. & Jarrard R.D., 1998. Petrophysics of core plugs from CRP-1 drillhole, Victoria Land Basin, Antarctica. In: Barrett P.J. & Ricci C.A. (eds.), *Studies from the Cape Roberts Project, Ross Sea, Antarctica - Scientific Report of CRP-1, Terra Antarctica*, **5**, 291-298.
- Brink J.D. & Jarrard R.D., 2000. Petrophysics of core plugs from CRP-2/2A drillhole, Victoria Land Basin, Antarctica. In: Barrett P.J. et al. (eds.), *Studies from the Cape Roberts Project, Ross Sea, Antarctica - Scientific Report of CRP-2/2A, Terra Antarctica*, **7**, 231-240.
- Bücker C.J., Jarrard R.D., Wonik T. & Brink J.D., 2000. Analysis of downhole logging data from CRP-2/2A, Victoria Land Basin, Antarctica: a multivariate statistical approach. In: Barrett P.J. et al. (eds.), *Studies from the Cape Roberts Project, Ross Sea, Antarctica - Scientific Report of CRP-2/2A, Terra Antarctica*, **7**, 299-309.
- Bücker C.J., Jarrard R.D., Niessen F. & Wonik T., 2001. Statistical analysis of wireline logging data of Cape Roberts Project Borehole CRP-3 (Victoria Land, Antarctica). This volume.
- Cape Roberts Science Team, 2000. *Studies from the Cape Roberts Project, Ross Sea, Antarctica, Initial Report on CRP-3. Terra Antarctica*, **7**, 1-209.
- Erickson S.N. & Jarrard R.D., 1998. Velocity-porosity relationships for water-saturated siliciclastic sediments. *J. Geophys. Res.*, **103**, 30385-30406.
- Gassmann F., 1951. Elastic waves through a packing of spheres. *Geophysics*, **16**, 673-685.
- Hamilton E.L., 1971a. Prediction of in situ acoustic and elastic properties of marine sediments. *Geophys.*, **36**, 266-284.
- Hamilton E.L., 1971b. Elastic properties of marine sediments. *J. Geophys. Res.*, **76**, 579-604.
- Hamilton E.L., 1976. Variations of density and porosity with depth in deep-sea sediments. *J. Sediment. Petrol.*, **46**, 280-300.
- Henrys S.A., Bücker C.J., Niessen F. & Bartek L.R., 2001. Correlation of seismic reflectors with the CRP-3 drillhole, Victoria Land Basin, Antarctica. This volume.
- Jarrard R.D., Dadey K. & Busch W., 1989. Velocity and density of sediments of Eirik Ridge, Labrador Sea: Control by porosity and mineralogy. *ODP Scientific Results*, **105**, 811-835.
- Jarrard R.D., Niessen F., Brink J.D. & Bücker C., 2000. Effects of cementation on velocities of siliciclastic sediments. *Geophys. Res. Lett.*, **27**, 593-596.
- Jarrard, R.D. & Schaar R.G., 1991. Electrical properties of oceanic crust at ODP Sites 768 and 770. *ODP Scientific Results*, **124**, 105-118.
- Jarrard R.D., Bücker C.J., Wilson T.J. & Paulsen T., 2001. Bedding dips from the CRP-3 drillhole, Victoria Land Basin, Antarctica. This volume.
- Jarrard R.D., Moos D., Wilson T.J., Bücker C.J. & Paulsen T.S., 2001. Stress patterns observed by borehole televiewer logging of the CRP-3 drillhole, Victoria Land Basin, Antarctica. This volume.
- Keller G.V., 1989. Electrical properties. In: Carmichael R.S. (ed.), *Practical Handbook of Physical Properties of Rocks and Minerals*, CRC Press, Boca Raton.
- Nur A., 1971. Effects of stress on velocity anisotropy in rocks with cracks. *J. Geophys. Res.*, **76**, 2022-2034.
- Nur A. & Murphy W., 1981. Wave velocities and attenuation in porous media with fluids. *Proc. 4th Int. Conf. on Continuum Models of Discrete Systems*, Stockholm, 311-327.
- Nur A., Marion D. & Yin H., 1991. Wave velocities in sediments. In: Hovem J.M., Richardson M.D. & Stoll R.D. (eds.), *Shear Waves in Marine Sediments*, Kluwer Acad., Norwell MA, 131-140.
- Porter C.R. & Carothers J.E., 1971. Formation factor – porosity relation derived from well log data. *The Log Analyst*, Jan-Feb, 16-26.
- Stoll R.D., 1989. *Sediment Acoustics*. Springer-Verlag, Berlin, 153 p.
- Walsh J.B., 1965. The effect of cracks on the compressibility of rock. *J. Geophys. Res.*, **70**, 381-389.
- Wise S.W., Jr., Smellie J.L., Aghib F.S., Jarrard R.D. & Krissek L.A., 2001. Authigenic smectite clay coats in CRP-3 drillcore, Victoria Land Basin, Antarctica, as a possible indicator of fluid flow: a progress report. This volume.
- Wyllie M.R.J., Gregory A.R. & Gardner G.H.F., 1958. An experimental investigation of factors affecting elastic wave velocities in porous media. *Geophysics*, **23**, 459-493.